UDC 621.3 https://doi.org/10.20998/2074-272X.2025.5.06

F. Senani, A. Rahab, H. Benalla

Performance evaluation and analysis by simulation for sliding mode control with speed regulation of permanent magnet synchronous motor drives in electric vehicles

Introduction. *This study introduces a sliding mode control (SMC) that utilizes multivariable system command estimation (MSCE-SMC) to create an innovative speed control system for the permanent magnet synchronous motor (PMSM). The motor operates through a 3-phase voltage source inverter when used in an electric vehicle (EV) model, with the goal of achieving fast speed regulation and high performance.* ***Problem.*** *The primary challenge is to achieve fast and accurate speed regulation for PMSMs while maintaining high performance, despite varying system parameters and external disturbances. The* ***goal*** *is to design a robust and adaptive speed control system for PMSMs using the SMC approach, which ensures precise speed tracking and high-performance regulation.* ***Scientific novelty.*** *The integration of MSCE-SMC approach, offering an innovative solution for speed control in PMSMs used in EVs.* ***Methodology.*** *SMC approach for the PMSM divides the system into 2 subsystems: electrical and speed. A d-q coordinate frame is used to model the PMSM, and its control strategy is outlined. A detailed model of the PMSM with SMC is presented after an in-depth review of the theoretical concepts and principles of sliding mode control.* ***Results.*** *To validate the proposed approach, MATLAB/Simulink is conducted, demonstrating the effectiveness and robustness of the method in PMSM speed regulation. The results confirm that the proposed method provides straightforward and precise control, accurate speed tracking, and high-performance regulation. It also shows adaptability to parameter variations and external disturbances.* ***Practical value.*** *The practical value of the proposed method is significant, as it provides a reliable and efficient control system for PMSMs. It offers precise speed control, robust performance under variable conditions, and high adaptability to external disturbances, making it suitable for real-world EV applications.* References 22, table 1, figures 18.

Key words: **permanent magnet synchronous motor, sliding mode control, electric vehicle, speed regulation**.

Вступ. *У дослідженні розглядається керування ковзним режимом (SMC), що використовує багатопараметричну оцінку системних команд (MSCE-SMC) для створення інноваційної системи керування швидкістю синхронного двигуна з постійними магнітами (PMSM). Двигун працює через трифазний інвертор напруги при використанні в моделі електромобіля (EV) з метою досягнення швидкого регулювання швидкості та високої продуктивності.* ***Проблема***. *Основне завдання полягає в досягненні швидкого і точного регулювання швидкості для PMSM при збереженні високої продуктивності, незважаючи на параметри системи, що змінюються, і зовнішні збурення.* ***Метою*** *є розробка надійної та адаптивної системи керування швидкістю для PMSM з використанням SMC підходу, що забезпечує точне відстеження швидкості та високопродуктивне регулювання.* ***Наукова новизна***. *Інтеграція підходу MSCE-SMC пропонує інноваційне рішення для управління швидкістю PMSM, що використовуються в EV.* ***Методологія***. *SMC підхід для PMSM поділяє систему на 2 підсистеми: електричну та швидкісну. Для моделювання PMSM використовується d-q система координат і описується стратегія його управління. Наведено докладну модель PMSM з SMC після поглибленого аналізу теоретичних концепцій та принципів управління в ковзному режимі.* ***Результати***. *Для перевірки пропонованого підходу проведено аналіз у середовищі MATLAB/Simulink, що показав ефективність та надійність методу регулювання швидкості PMSM. Результати підтверджують, що запропонований метод забезпечує просте і точне керування, коректне відстеження швидкості та високопродуктивне регулювання. Він також демонструє адаптивність до змін параметрів та зовнішніх збурень.* ***Практична цінність*** *запропонованого методу значна, оскільки він забезпечує надійну та ефективну систему управління PMSM. Він забезпечує точне управління швидкістю, надійну роботу в змінних умовах, і високу адаптивність до зовнішніх збурень, що робить його придатним для застосування в реальних EV.* Бібл. 22, табл. 1, рис. 18.

Ключові слова: **синхронний двигун з постійними магнітами, керування ковзним режимом, електромобіль, регулювання швидкості.**

Introduction. Electric vehicles (EVs) that use electric motors are used to replace traditional gasoline vehicles that use internal combustion engines in order to reach the level of emissions of fossil fuels [1–4]. permanent magnet synchronous motor (PMSM) in recent years have played an increasingly important role in many industrial applications due to the advances in magnetic materials, recent technological developments in power electronics and control theories [5]. Due to their high torque-power density, high efficiency and low maintenance, PMSM-based drive is also becoming widely used in EVs [6, 7]. There are various nonlinear command methods have been proposed to improve the command performance of PMSM, such as sliding mode control (SMC), adaptive control, predictive control [8, 9], intelligent control, etc. Field-oriented control based conventional PI method is difficult to deal with loud disturbances, variations parameters and cannot adapt to the applications of high-precision control [10]. SMC has attracted many researchers in recent years. High-frequency switching devices and high-performance microprocessors have contributed to the recent increase in interest in this command method [11]. The effectiveness of this solution is attributed to its distinct advantages, including insensitivity to parameter variations, rapid dynamic response and the ability to reject external disturbances [12].

SMC is a particular mode of operation of systems with variable structure [13]. The theory of these systems was studied and developed in the USSR first by S.V. Emelyanov, then by other collaborators such as V.I. Utkin based on the work of the mathematician A.F. Filippov on differential equations with discontinuous second member. Then the work was taken up elsewhere: in the US by Prof. Slotine, and in Japan by Prof. Young, Prof. Harishama and Prof. Hashimoto. In SMC, the command switches between two different values according to the sign of a switching function (called switching or sliding surface) defined in the state space of the system [14]. This is introduced in order to obtain better stability, and high precision than those generally obtained by classical regulators [15, 16]. Several approaches exist for the choice of the sliding surface. In this work, we are interested in the study of an approach that considers a nonlinear surface [17, 18], the synthesis of which is based on Lyapunov stability theory. The strong robustness,

simplicity and ease of implementation make it an ideal choice for high performance by regularly adjusting the system structure to combat parameter variations and external disturbances [19, 20].

The **goal** of the article is to design a robust and adaptive speed control system for PMSMs using the SMC approach, which ensures precise speed tracking and high-performance regulation. The proposed controller is investigated and analyzed in different control speeds, load conditions, and rotational speed direction.

Model of PMSM. The model of PMSM in *d-q* frame is represented by equations: electrical, magnetic, and electromagnetic. The stator voltages equations expressed as [21]:

$$V_d = RI_d + \frac{\mathrm{d}\varphi_d}{dt} - \omega\varphi_q\,; \tag{1}$$

$$V_q = RI_q + \frac{\mathrm{d}\varphi_q}{\mathrm{d}t} + \omega\varphi_d\,, \tag{2}$$

where V_d, V_q, φ_d, φ_q, I_d, I_q are the direct and quadrature axis of voltages, fluxes and currents respectively; R is the stator resistance; ω is the mechanical angular speed.

The stator flux equations expressed [21]:

$$\varphi_d = L_d I_d + \varphi_m\,; \tag{3}$$

$$\varphi_q = L_q I_q\,, \tag{4}$$

where L_d, L_q, are the direct and quadrature stator inductances; φ_m is the constant permanent magnet flux.

The PMSM model equations in *d-q* axis expressed as:

$$V_d = RI_d + L_d\frac{\mathrm{d}I_d}{\mathrm{d}t} - \omega L_q I_q\,; \tag{5}$$

$$V_q = RI_q + L_q\frac{\mathrm{d}I_q}{\mathrm{d}t} + \omega(L_d I_d + \varphi_m)\,. \tag{6}$$

The expression for electromagnetic torque T_e [21] is:

$$T_e = P((L_d - L_q)I_q L_d + I_q\varphi_m)\,. \tag{7}$$

PMSM is assumed to surface mounted PMSM ($L_d = L_q = L$) the electromagnetic torque becomes:

$$T_e = pI_q\varphi_m\,, \tag{8}$$

where T_e is the electromagnetic torque; p is the number of pole pairs.

The expression of the mechanical equation [21] is:

$$J\frac{\mathrm{d}\omega_m}{\mathrm{d}t} + f_v\omega_m = T_e - T_L\,, \tag{9}$$

where J is the moment of inertia; T_L is the load torque; f_v is the viscous friction coefficient; ω_m is the rotor mechanical speed of the PMSM.

SMC theory. Variable structure systems can be controlled using SMC. Three different parts make up the trajectory (Fig. 1): the convergence mode (CM), the sliding mode (SM) and the permanent mode (PM) [22].

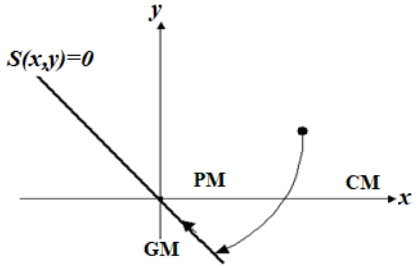

Fig. 1 Different modes trajectory of the SMC

The choice of the surface. The design of SMC was executed in 3 key phases [22]: selection of the surface, conditions necessary for convergence, meaning of the control law. The sliding surfaces choice is shaped by the number and shape of required functions. The control vector $\boldsymbol{u}$ and surface vector have the same dimension defined by:

$$\dot{x} = A(x,t)x + B(x,t)u\,. \tag{10}$$

The nonlinear form depends on the error in the variable to be regulated, known as x:

$$S(x) = \left(\frac{\partial}{\partial t} + \lambda_x\right)^{r-1} e(x)\,, \tag{11}$$

where $e(x)$ is the difference between the variable to be adjusted and its reference: $e(x) = x^* - x$; λ_x is the positive constant; r is the relative degree and indicates the number of times the surface needs to be differentiated to show control.

The SMC objective is to maintain the surface at zero. The only possible solution for this surface is $e(x) = 0$, which a linear differential equation.

Convergence and existence conditions. Two considerations to ensure convergence mode [22], the discreet switching function (it is proposed and studied by S.V. Emelyanov and V.I. Utkin):

$$\begin{cases}\dot{S}(x) > 0 \;\text{ if }\; S(x) < 0;\\ \dot{S}(x) < 0 \;\text{ if }\; S(x) > 0.\end{cases} \tag{12}$$

This condition can be formulated in another way:

$$\dot{S}(x)S(x) < 0\,. \tag{13}$$

The Lyapunov function defines as follows:

$$V(x) = \frac{1}{2}S^2(x)\,. \tag{14}$$

The derivative of this function is:

$$\dot{V}(x) = S(x)\dot{S}(x)\,. \tag{15}$$

Calculation of the control. The SMC structure consists of the exact linearization (u_{eq}) and the other stabilizing (u_n) [22]:

$$u = u_{eq} + u_n. \tag{16}$$

In order to illustrate the previous development, we will consider a system that is described in the state space by (10). The aim is to establish the equivalent expression for the control input u.

The derivative of the surface is:

$$\dot{S}(x) = \frac{\partial S}{\partial t} = \frac{\partial S}{\partial x}.\frac{\partial x}{\partial t}\,. \tag{17}$$

Replacing (10) and (16) in (17), we find:

$$\dot{S}(x) = \frac{\partial S}{\partial x}\left(A(x,t) + B(x,t)u_{eq}\right) + \frac{\partial S}{\partial x}B(x,t)u_n\,. \tag{18}$$

Equivalent command's expression:

$$u_{eq} = -\left(\frac{\partial S}{\partial x}B(x,t)\right)^{-1}\frac{\partial S}{\partial x}A(x,t)\,. \tag{19}$$

For the equivalent control to take a finite value, it is necessary that $\frac{\partial S}{\partial x}B(x,t) \neq 0$.

Substituting the equivalent control with its expression from (18) in convergence mode we obtain:

$$\dot{S}(x,t) = \frac{\partial S}{\partial x}B(x,t)u_n\,. \tag{20}$$

Attractiveness condition expressed by (13) becomes:

$$S(x,t)\frac{\partial S}{\partial x}B(x,t)u_{eq}. \qquad (21)$$

In order to satisfy this condition, the sign of a must be opposite to that of $S(x,t)\frac{\partial S}{\partial x}B(x,t)$.

The simplest form that discrete control (Fig. 2):

$$u_n = K\cdot\text{sign}(S(x,t)), \qquad (22)$$

where the sign K must be different from that $\frac{\partial S}{\partial x}B(x,t)$.

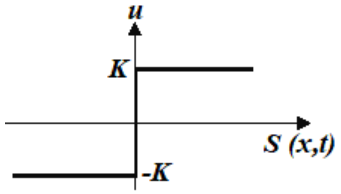

Fig. 2. Representation of discontinuous control

Application the SMC for the speed command of PMSM drive EV. The model of the PMSM, whose state variables are the stator currents and the mechanical speed [21]:

$$\begin{cases} \frac{dI_d}{dt} = -\frac{R}{L_d}I_d + \omega\frac{L_q}{L_d}I_q + \frac{1}{L_d}V_d; \\ \frac{dI_q}{dt} = -\frac{R}{L_q}I_q - \omega\frac{L_d}{L_q}I_d - \frac{\omega}{L_q}\varphi_m + \frac{1}{L_q}V_q; \\ \frac{d\omega_m}{dt} = \frac{1}{J}p\varphi_m I_q - \frac{1}{J}T_L - \frac{f_v}{J}\omega_m. \end{cases} \qquad (23)$$

The diagram of the SMC for the PMSM drive in an EV (Fig. 3) includes 3 surfaces.

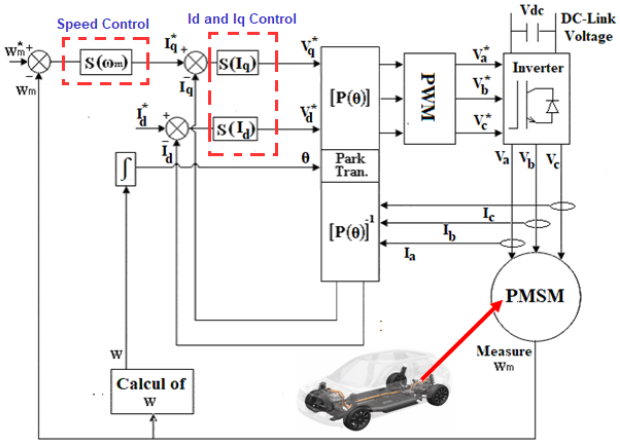

Fig. 3. Diagram of SMC for PMSM drive an EV

Speed control surface ω_m. Speed control surface has the form:

$$S(\omega_m) = \omega_m^* - \omega_m. \qquad (24)$$

The derivative of the surface is:

$$\dot{S}(\omega_m) = \dot{\omega}_m^* - \dot{\omega}_m. \qquad (25)$$

The equation (25) becomes:

$$\dot{S}(\omega_m) = \dot{\omega}_m^* - \left[\frac{1}{J}p\varphi_m I_q - \frac{1}{J}T_L - \frac{f_v}{J}\omega_m\right]. \qquad (26)$$

By replacing the current I_q with the control current $I_q = I_{qeq} + I_{qn}$, equation (26) can be written as:

$$\dot{S}(\omega_m) = \dot{\omega}_m^* - \left[\frac{1}{J}p\varphi_m I_{qeq} + \frac{1}{J}p\varphi_m I_{qn} - \frac{1}{J}T_L - \frac{f_v}{J}\omega_m\right]. \qquad (27)$$

We have $S(\omega_m) = 0$ and consequently $\dot{S}(\omega_m) = 0$ and $I_{qn} = 0$, the equivalent order I_{qeq}:

$$I_{qeq} = \frac{J}{p\varphi_m}\left[\frac{f_v}{J}\omega_m + \frac{1}{J}T_L\right]. \qquad (28)$$

The condition $\dot{S}(\omega_m)S(\omega_m) < 0$ must be checked. Substituting (28) in (27), we find:

$$\dot{S}(\omega_m) = \dot{\omega}_m^* - \frac{1}{J}p\varphi_m I_{qn}. \qquad (29)$$

By choosing the discontinuous control form (Fig. 2), we therefore pose:

$$I_{qn} = K_\omega \text{sign}(S(\omega_m)). \qquad (30)$$

Current quadrature control surface I_q. Current quadrature control surface has the form:

$$S(I_q) = I_q^* - I_q. \qquad (31)$$

The derivative of this surface is:

$$\dot{S}(I_q) = \dot{I}_q^* - \dot{I}_q. \qquad (32)$$

Taking into account the expression of $\dot{I}_q$ given by the system (23), the equation (32) becomes:

$$\dot{S}(I_q) = \dot{I}_q^* - \left[-\frac{R}{L_q}I_q - \omega\frac{L_d}{L_q}I_d - \frac{\omega}{L_q}\varphi_m + \frac{1}{L_q}V_q\right]. \qquad (33)$$

By replacing the voltage V_q with the control voltage $V_q = V_{qeq} + V_{qn}$, we find:

$$\dot{S}(I_q) = \dot{I}_q^* - \left[-\frac{R}{L_q}I_q - \omega\frac{L_d}{L_q}I_d - \frac{\omega}{L_q}\varphi_m + \frac{1}{L_q}V_{qeq} + \frac{1}{L_q}V_{qn}\right]. \qquad (34)$$

We have $S(I_q) = 0$ and consequently $\dot{S}(I_q) = 0$ and $V_{qn} = 0$, the equivalent order V_{qeq}:

$$V_{qeq} = RI_q + \omega L_d I_d + \omega\varphi_m. \qquad (35)$$

The condition $\dot{S}(I_q)S(I_q) < 0$ must be checked. Substituting (35) in (34), we find:

$$\dot{S}(I_q) = \frac{1}{L_q}V_{qn}. \qquad (36)$$

We therefore pose:

$$V_{qn} = K_q \text{sign}(S(I_q)). \qquad (37)$$

Current direct control surface I_d. Current direct control surface has the form:

$$S(I_d) = I_d^* - I_d. \qquad (38)$$

The derivative of this surface is:

$$\dot{S}(I_d) = \dot{I}_d^* - \dot{I}_d. \qquad (39)$$

Taking into account the expression of $\dot{I}_d$ given by the system (23), the equation (39) becomes:

$$\dot{S}(I_d) = \dot{I}_d^* - \left[-\frac{R}{L_d}I_d + \omega\frac{L_q}{L_d}I_q + \frac{1}{L_d}V_d\right]. \qquad (40)$$

By replacing the V_d with $V_d = V_{deq} + V_{dn}$, we find:

$$\dot{S}(I_d) = \dot{I}_d^* - \left[-\frac{R}{L_d}I_d + \omega\frac{L_q}{L_d}I_q + \frac{1}{L_d}V_{deq} + \frac{1}{L_d}V_{dn}\right]. \qquad (41)$$

We have $S(I_d) = 0$ and consequently $\dot{S}(I_d) = 0$ and $V_{dn} = 0$, from which we derive the equivalent order V_{deq}:

$$V_{deq} = RI_d + \omega L_q I_q . \quad (42)$$

The condition $\dot{S}(I_d)S(I_d) < 0$ must be checked. Substituting (42) in (41), we find:

$$\dot{S}(I_d) = \frac{1}{L_d} V_{dn} . \quad (43)$$

We therefore pose:

$$V_{dn} = K_d \text{sign}(S(I_d)) . \quad (44)$$

Simulation results of speed regulation of PMSM-SMC. SMC for PMSM powered voltage source inverter for a model EV has been implemented in MATLAB/Simulink. A constant reference flux (φ_{mref} = 0.12 Wb) is used to conduct the simulations. In this set of simulation, a load variation is added when the PMSM is under the speed regulation, and the operating speed is 157 rad/s. PMSM is considered in the simulation and parameters as given in Table 1.

Table 1

PMSM parameters

Parameters	Values
Rated power	1.5 kW
Frequency	50 Hz
Rotor speed	1500 rpm / 157 rad/s
Stator resistance	0.18 Ω
Inductance *d* axis	2.1 mH
Inductance *q* axis	4.2 mH
Moment of inertia	0.0066 kg·m^2
Viscous friction coefficient	0.0014 N·s/rad
Constant rotor flux linkage	0.12 Wb
Number of pole pairs	2

Simulation for successive step changes in reference speed under full load conditions (Fig. 4–8). We involve sequential step change in control speed under full load conditions. The PMSM is initially started at 83.5 rad/s step control speed. At t = 1 s, a step-up change occurs, increasing the control speed from 83.5 rad/s to 104.5 rad/s. Finally, at t = 2 s, another change the command speed from 104.5 rad/s to 157 rad/s.

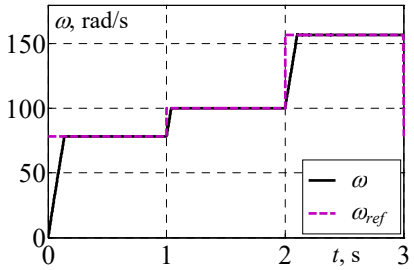

Fig. 4. Reference speed and PMSM speed

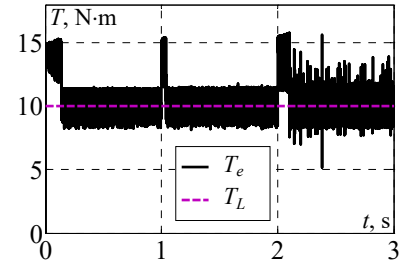

Fig. 5. Electromagnetic torque and load torque

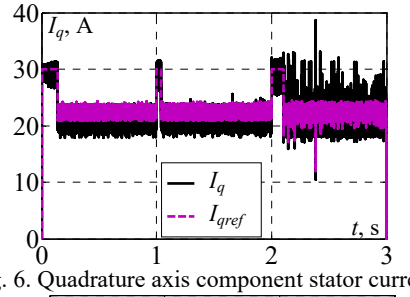

Fig. 6. Quadrature axis component stator current

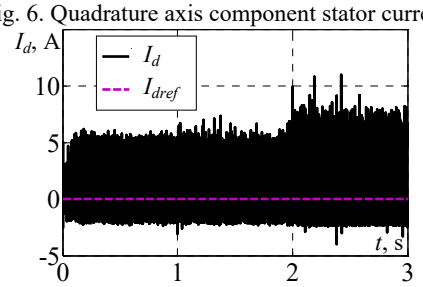

Fig. 7. Direct axis component stator current

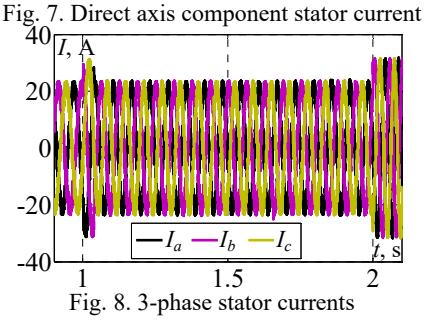

Fig. 8. 3-phase stator currents

Simulation for reference speed fix and step change of load (Fig. 9–13). In this part, the PMSM is under speed control 157 rad/s with a load variation at t = 1 s, the load torque changes from 10 N·m to 5 N·m and at t = 2 s another change the load torque changes from 5 N·m to 10 N·m.

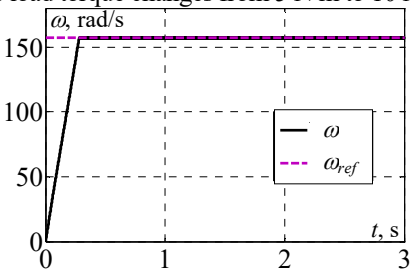

Fig. 9. Reference speed and PMSM speed

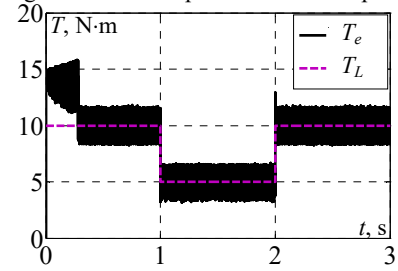

Fig. 10. Electromagnetic torque and load torque

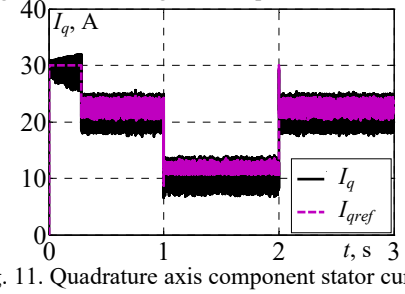

Fig. 11. Quadrature axis component stator current

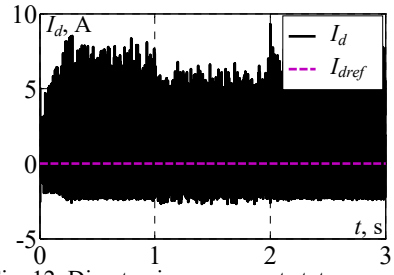

Fig. 12. Direct axis component stator current

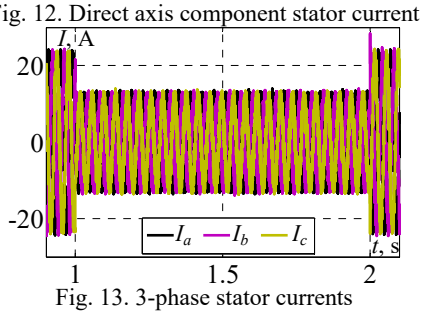

Fig. 13. 3-phase stator currents

Simulation for reference speed and inverse speed and under full load (Fig. 14–18). We apply a full load start of PMSM (T_L = 10 N·m) until at t = 1 s. The speed reference is equal to the synchronism speed 157 rad/s until t = 1.5 s, then the direction of rotation is reversed at a speed –157 rad/s.

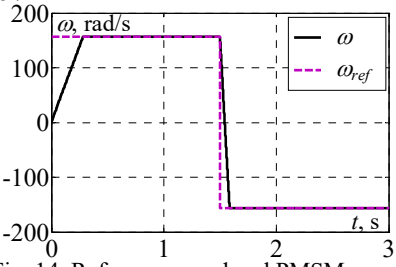

Fig. 14. Reference speed and PMSM speed

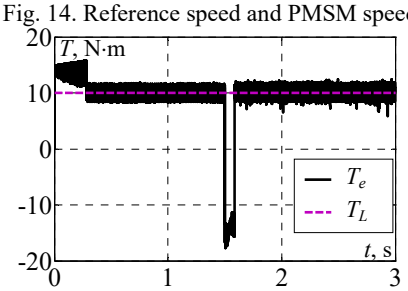

Fig. 15. Electromagnetic torque and load torque

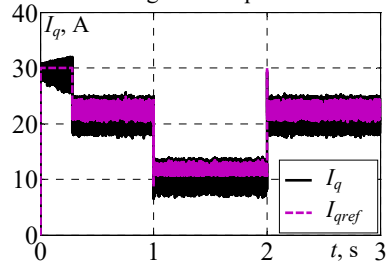

Fig. 16. Quadrature axis component stator current

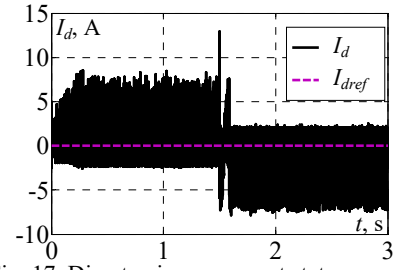

Fig. 17. Direct axis component stator current

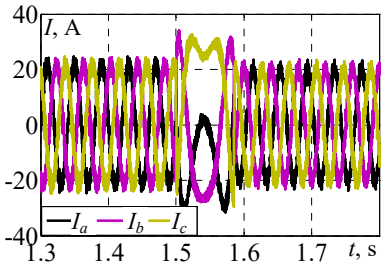

Fig. 18. 3-phase stator currents

Discussions of results. In Fig. 4, 9, 14, the speed of PMSM obtained with SMC the speed appears to be consistent, with the real speed closely mirroring the command speed. The system responds efficiently to changes in command speed and exhibits a smooth rise time from 104.5 rad/s to 157 rad/s. Analyzing the difference between command and real speeds at each stage is crucial to gain insight into the system's performance and potential limitations. In these cases, the rise time indicates how responsive the system is, and shorter rise times generally mean better control dynamics and faster adaptation to command input changes and settling time is satisfying in tree case seamlessly traced the speed reference without exceeding; in Fig. 9 rotation speed equal to rotation speed 157 rad/s seamlessly traced the speed reference without exceeding; in Fig. 14 with a positive speed command of 157 rad/s, speed response with the SMC neatly settled at the reference. Sudden reference speed reversal from 157 rad/s to –157 rad/s leading to change in speed orientation for the 2 models at –157 rad/s, the SMC seamlessly traced the speed reference without exceeding.

The load torque and electromagnetic torque are matched in Fig. 5, 10, 15 by SMC. The electromagnetic torque is kept constant during the speed build-up phase to ensure acceleration. The electromagnetic torque will decrease to 5 N·m once the rotor speed matches the reference speed. This equilibrium is achieved faster in the SMC model due to the absence of speed overshoot. The electromagnetic torque closely tracks the load torque, except during brief intervals when the speed increases (Fig. 5) or reverses (Fig. 15). These deviations are minimal and occur over very short periods.

In Fig. 6, 11, 16, the quadrature component of the stator current are compared with the quadrature component current reference; is in direct proportion to electromagnetic torque T_e.

In Fig. 7, 12, 17, the direct component of the stator current is compared with the direct component current reference is met at zero.

In Fig. 8, 13, 18 the stator 3-phase currents (*abc*) are shown. When as the PMSM speed rises, the frequency of the current waveform also increases (Fig. 8) and when the load torque decreases from its nominal value (5 N·m) to 3 N·m of the current waveform also decreases (Fig. 15).

Conclusions. This paper describes the creation and execution of speed controllers that use SMC-based technology in a SMC drive structure for a PMSM in an EV drive. The SMC algorithm's speed control loop uses a sliding mode controller based on surface dynamics instead of the traditional PI controller in the outer control

loop. Applied MATLAB/Simulink software was utilized to conduct simulation analyses and evaluations to assess the performance and effectiveness of the SMC for PMSM. The proposed system's dynamic response was tested under different reference speeds, load conditions, and reverse speed scenarios.

The simulation results show that the SMC can perform dynamically quickly and accurately, without any overshoot, minimal steady-state error, and a short rise time, which is superior for PMSM speed control applications. SMC is characterized by its significant torque ripple, which remains a major concern.

Conflict of interest. The authors declare that they have no conflicts of interest.

REFERENCES

1. Liu F., Wang X., Xing Z. Design of a 35 kW Permanent Magnet Synchronous Motor for Electric Vehicle Equipped With Non-Uniform Air Gap Rotor. *IEEE Transactions on Industry Applications*, 2023, vol. 59, no. 1, pp. 1184-1198. doi: https://doi.org/10.1109/TIA.2022.3206258.

2. Ibrar A., Ahmad S., Safdar A., Haroon N. Efficiency enhancement strategy implementation in hybrid electric vehicles using sliding mode control. *Electrical Engineering & Electromechanics*, 2023, no. 1, pp. 10-19. doi: https://doi.org/10.20998/2074-272X.2023.1.02.

3. Boumegouas M.K.B., Kouzi K. A New Synergetic Scheme Control of Electric Vehicle Propelled by Six-phase Permanent Magnet Synchronous Motor. *Advances in Electrical and Electronic Engineering*, 2022, vol. 20, no. 1, pp. 1-14. doi: https://doi.org/10.15598/aeee.v20i1.4221.

4. Wang Z., Ching T.W., Huang S., Wang H., Xu T. Challenges Faced by Electric Vehicle Motors and Their Solutions. *IEEE Access*, 2021, vol. 9, pp. 5228-5249. doi: https://doi.org/10.1109/ACCESS.2020.3045716.

5. Patel A.N., Doshi P.J., Mahagoakar S.C., Panchal T.H. Optimization of cogging torque in interior permanent magnet synchronous motor using optimum magnet v-angle. *Electrical Engineering & Electromechanics*, 2023, no. 6, pp. 16-20. doi: https://doi.org/10.20998/2074-272X.2023.6.03.

6. Mazzi Y., Ben Sassi H., Errahimi F., Es-Sbai N. Speed Control of a PMSM drive system using a nonsingular terminal sliding mode controller. *Statistics, Optimization & Information Computing*, 2024, vol. 13, no. 1, pp. 450-458. doi: https://doi.org/10.19139/soic-2310-5070-1913.

7. Djafer L., Taleb R., Mehedi F., Aissa Bokhtache A., Bessaad T., Chabni F., Saidi H. Electric drive vehicle based on sliding mode control technique using a 21-level asymmetrical inverter under different operating conditions. *Electrical Engineering & Electromechanics*, 2025, no. 3, pp. 31-36. doi: https://doi.org/10.20998/2074-272X.2025.3.05.

8. Loro J.A.R. Robust Position Control of SM-PMSM Based on a Sliding Mode Current Observer. *International Journal of Electrical and Electronic Engineering & Telecommunications*, 2020, vol. 9, no. 5, pp. 337-341. doi: https://doi.org/10.18178/ijeetc.9.5.337-341.

9. Chen Y., Li M., Gao Y., Chen Z. A sliding mode speed and position observer for a surface-mounted PMSM. *ISA Transactions*, 2019, vol. 87, pp. 17-27. doi: https://doi.org/10.1016/j.isatra.2018.11.011.

10. Varatharajan A., Pellegrino G., Armando E. Direct Flux Vector Control of Synchronous Motor Drives: A Small-Signal Model for Optimal Reference Generation. *IEEE Transactions on Power Electronics*, 2021, vol. 36, no. 9, pp. 10526-10535. doi: https://doi.org/10.1109/TPEL.2021.3067694.

11. Awan H.A.A., Hinkkanen M., Bojoi R., Pellegrino G. Stator-Flux-Oriented Control of Synchronous Motors: A Systematic Design Procedure. *IEEE Transactions on Industry Applications*, 2019, vol. 55, no. 5, pp. 4811-4820. doi: https://doi.org/10.1109/TIA.2019.2927316.

12. Lin H., Lee K., Kim S., Ahn H., You K. Speed Regulation for PMSM using a Novel Sliding Mode Controller. *Journal of Multidisciplinary Engineering Science and Technology (JMEST)*, 2021, vol. 8, no. 12, pp. 11842-11845.

13. Wang Q., Wang S., Chen C. Review of sensorless control techniques for PMSM drives. *IEEJ Transactions on Electrical and Electronic Engineering*, 2019, vol. 14, no. 10, pp. 1543-1552. doi: https://doi.org/10.1002/tee.22974.

14. Zhang X., Sun L., Zhao K., Sun L. Nonlinear Speed Control for PMSM System Using Sliding-Mode Control and Disturbance Compensation Techniques. *IEEE Transactions on Power Electronics*, 2013, vol. 28, no. 3, pp. 1358-1365. doi: https://doi.org/10.1109/TPEL.2012.2206610.

15. Zhang W., Kong J. A novel fast and chattering-free speed control method for PMSM motor drive based on sliding mode control. *International Journal of Dynamics and Control*, 2024, vol. 12, no. 9, pp. 3332-3338. doi: https://doi.org/10.1007/s40435-024-01419-2.

16. Kim H., Son J., Lee J. A High-Speed Sliding-Mode Observer for the Sensorless Speed Control of a PMSM. *IEEE Transactions on Industrial Electronics*, 2011, vol. 58, no. 9, pp. 4069-4077. doi: https://doi.org/10.1109/TIE.2010.2098357.

17. Chi S., Zhang Z., Xu L. Sliding-Mode Sensorless Control of Direct-Drive PM Synchronous Motors for Washing Machine Applications. *IEEE Transactions on Industry Applications*, 2009, vol. 45, no. 2, pp. 582-590. doi: https://doi.org/10.1109/TIA.2009.2013545.

18. Junejo A.K., Xu W., Mu C., Ismail M.M., Liu Y. Adaptive Speed Control of PMSM Drive System Based a New Sliding-Mode Reaching Law. *IEEE Transactions on Power Electronics*, 2020, vol. 35, no. 11, pp. 12110-12121. doi: https://doi.org/10.1109/TPEL.2020.2986893.

19. Dandan S., Yugang D., Chengning Z. Sliding Mode Controller for Permanent Magnetic Synchronous Motors. *Energy Procedia*, 2017, vol. 105, pp. 2641-2646. doi: https://doi.org/10.1016/j.egypro.2017.03.765.

20. Fallaha C.J., Saad M., Kanaan H.Y., Al-Haddad K. Sliding-Mode Robot Control With Exponential Reaching Law. *IEEE Transactions on Industrial Electronics*, 2011, vol. 58, no. 2, pp. 600-610. doi: https://doi.org/10.1109/TIE.2010.2045995.

21. Guezi A., Bendaikha A., Dendouga A. Direct torque control based on second order sliding mode controller for three-level inverter-fed permanent magnet synchronous motor: comparative study. *Electrical Engineering & Electromechanics*, 2022, no. 5, pp. 10-13. doi: https://doi.org/10.20998/2074-272X.2022.5.02.

22. Senani F., Rahab A., Benalla H. Squirrel Cage Induction Motor (SCIM) Rotor Flux Estimation and Observer Using Multivariable Sliding Mode Control (MSMC). *Algerian Journal of Signals and Systems*, 2024, vol. 9, no. 2, pp. 121-127. doi: https://doi.org/10.51485/ajss.v9i2.219.

Received 16.02.2025
Accepted 29.04.2025
Published 02.09.2025

F. Senani[1,2]*, PhD in Electrical Engineering, Associate Professor,*
A. Rahab[1,2]*, PhD in Electrical Engineering, Associate Professor,*
H. Benalla[2]*, PhD in Electrical Engineering, Professor,*
[1] Higher Normal School of Technological Education of Skikda (ENSET Skikda), Technology Department, Algeria,
e-mail: senani.fouzi@gmail.com (Corresponding Author);
rahababderezzak@gmail.com
[2] Electrotechnical Laboratory of Constantine (LEC),
Department of Electrical Engineering,
Faculty of Science and Technology,
University of Constantine 1, Algeria,
e-mail: benalladz@yahoo.fr

How to cite this article:
Senani F., Rahab A., Benalla H. Performance evaluation and analysis by simulation for sliding mode control with speed regulation of permanent magnet synchronous motor drives in electric vehicles. *Electrical Engineering & Electromechanics*, 2025, no. 5, pp. 43-48. doi: https://doi.org/10.20998/2074-272X.2025.5.06